## Quantum and Classical Proton Diffusion in Superconducting Clathrate Hydrides

Hui Wang<sup>1,†</sup>, Yansun Yao<sup>2</sup>, Feng Peng<sup>3</sup>, Hanyu Liu<sup>4,5,‡</sup> and Russell J. Hemley<sup>6</sup>

<sup>1</sup>Key Laboratory for Photonic and Electronic Bandgap Materials, Ministry of Education, School of Physics and
Electronic Engineering, Harbin Normal University, Harbin 150025, China

<sup>2</sup>Department of Physics and Engineering Physics, University of Saskatchewan,

Saskatoon, Saskatchewan S7N 5E2, Canada

<sup>3</sup>College of Physics and Electronic Information, Luoyang Normal University, Luoyang 471022, P. R. China <sup>4</sup>International Center for Computational Method & Software, College of Physics,

Jilin University, Changchun 130012, China

<sup>5</sup>Key Laboratory of Physics and Technology for Advanced Batteries (Ministry of Education) and State Key Laboratory of Superhard Materials, College of Physics, International Center of Future Science,

Jilin University, Changchun 130012, China

<sup>6</sup>Departments of Physics and Chemistry, University of Illinois at Chicago, Chicago, IL 60607, USA

The discovery of near room temperature superconductivity in clathrate hydrides has ignited the search for both higher temperature superconductors and deeper understanding of the underlying physical phenomena. In a conventional electron-phonon mediated picture for the superconductivity for these materials, the high critical temperatures predicted and observed can be ascribed to the low mass of the protons, but this also poses nontrivial questions associated with how the proton dynamics affect the superconductivity. Using clathrate superhydride Li<sub>2</sub>MgH<sub>16</sub> as an example, we show through *ab initio* path integral simulations that proton diffusion in this system is remarkably high, with a diffusion coefficient for example reaching 6×10<sup>-6</sup> cm<sup>2</sup>/s at 300 K and 250 GPa. The diffusion is achieved primarily through proton transfer among interstitial voids within the otherwise rigid Li<sub>2</sub>Mg sublattice at these conditions. The findings indicate the coexistence of proton quantum diffusion together with hydrogen-induced superconductivity, with implications for other very high temperature superconducting hydrides.

Superconductivity at - and even above - room temperature is among the most fascinating phenomena in condensed matter physics. First suggested by early predictions for atomic metallic hydrogen[1], it is now of great interest as a result of recent breakthroughs in studies of hydrogen-rich materials under pressure. It is understood that when a system has very high phonon vibrational frequencies, as in materials containing a great deal of hydrogen, even moderate coupling of these phonons to electron motions could result in a high superconducting  $T_c$  [1,2]. With its origins in Bardeen-Cooper-Schrieffer (BCS) theory [3], this principle has been substantiated by *ab initio* calculations and theoretical design of a large variety of H-rich hydrides [4,5] together with the experimental realization of both the predicted H-rich structures and high- $T_c$  behavior of a growing number of H-hydrides (see Refs. [6-8]. In particular, the observations of record high- $T_c$  superconductivity of 203 K in H<sub>3</sub>S [9] and near room temperature in LaH<sub>10</sub>-based superhydride [10,11], followed by later studies of the Y-H system [12,13] have confirmed predictions [14,15]. Indeed, the  $T_c$  onset of superconductivity in a C-S-H mixture recently reported to reach room temperature at higher pressures [16] is also in accord with theoretical predictions [17,18].

In addition to electron-phonon coupling (EPC), a singular feature of both solid hydrogen [19] and H-rich hydrides is the appreciable dynamical properties of the nuclei over a broad range of temperatures. This strong dynamics underlie predictions that compressed hydrogen could be a unique two-component system of protons and electrons exhibiting unique superconducting fluid and superconducting superfluid behavior at sufficiently high pressures [20]. Manifestations of such quantum dynamical properties are presaged in the molecular phases of dense hydrogen that have been characterized to date. For example, in the high-pressure phase IV of hydrogen, fluxional sublattice proton transfer within its graphene-like sheets of short-lived H<sub>2</sub> predicted by *ab initio* simulations [21] is consistent with experiment [22-24]. The phase is considered an important intermediate between molecular and atomic phases of dense solid hydrogen. Since H-rich hydrides also contain a large proportion of hydrogen, proton quantum dynamics in these materials merit

investigation not considered previously, in particular, to reveal its influence on superconductivity, both predicted for pure hydrogen and now observed in superhydrides.

Clathrate hydrides are three-dimensional extended cage structures of atomic hydrogen, analogous to atomic metallic hydrogen in both the atomic environment, orbital hybridization, and proposed EPC mechanism [25,26]. In some clathrate hydrides, the large cages of hydrogen are formed by more than one crystallographic sites, e.g. H<sub>29</sub> cages in YH<sub>9</sub> and H<sub>32</sub> cages in LaH<sub>10</sub> [14]. The difference in site symmetry imparts dynamical behavior of the corresponding protons, leading to potential classical and quantum diffusion between sites, analogous to the behavior of protons in hydrogen phase IV. The coexistence of appreciable proton diffusion and superconductivity in very high-T clathrate hydrides is therefore a real possibility. This scenario is reminiscent of the two-component superconducting fluid proposed for hydrogen condensates in strong magnetic fields [20]. The extent to which proton diffusion breaks or otherwise modifies the EPC in very high  $T_c$  superconducting clathrate hydrides is thus an important question.

To address this problem and to illustrate the effect, we focused on Li<sub>2</sub>MgH<sub>16</sub> [27] as a model system because of its very high predicted  $T_c$  based on the theoretical schemes that led to discoveries of high- $T_c$  hydrides H<sub>3</sub>S, LaH<sub>10</sub>, and the Y-H superconductors. In Li<sub>2</sub>MgH<sub>16</sub>, the hydrogen atoms form a clathrate framework consisting of face-shared H<sub>28</sub> cages with nearest H-H distances of 1.02-1.23 Å at 250-300 GPa (Fig. 1a). At these pressures, the material is calculated to have very high  $T_c$ 's with a large variation (330-473 K), which provides a wide P-T range for exploring the classical and quantum proton diffusion and its effects on superconductivity in the clathrate H framework. In Li<sub>2</sub>MgH<sub>16</sub> the Li and Mg atoms are arranged in a C15 cubic Laves sublattice in which the Mg atoms form a diamond structure with the four tetrahedral voids occupied by Li tetrahedra. All interstitial sites in this sublattice are tetrahedral, and thus grouped in g, e, and b Wyckoff sites and coordinated by [Li<sub>2</sub>Mg<sub>2</sub>], [Li<sub>3</sub>Mg], and [Li<sub>4</sub>] tetrahedra, respectively (Fig. 1). Notably, unusual proton dynamics in isolated hexagons formed by nearest g sites has been

documented experimentally in C15-Laves hydride solutions [28,29]. Localized hopping of protons within single hexagons was found at low temperatures (as low as 30 K), but at room temperature, the proton motion evolves toward long-range diffusion across neighboring hexagons. In  $\text{Li}_2\text{MgH}_{16}$ , the clathrate H framework has fully occupied g and e sites, whereas the b sites are empty; therefore different proton dynamics are expected.

To further probe the proton motion in  $Li_2MgH_{16}$ , we derived the occupation numbers of the g, e, and b sites at different temperatures from NVT trajectories of 2 ps at 20 fs intervals at 250 and 300 GPa (Figs. 2a and 2b). At 250 GPa, a moderate g-b redistribution of proton density is seen at all temperatures at the beginning of the trajectory. This process appears to be intrinsic; i.e., the g tetrahedra are sufficiently large that even zero-point vibrations can set off the enclosed protons and transfer them to empty sites in the structure. In contrast, at 300 GPa, the g-b redistribution only occurs at temperatures greater than 25 K, indicating that the g tetrahedra are now reduced and hold the protons more tightly so only those with sufficient kinetic energy can break through. The e site is midway between the g and b sites, and therefore acts as a channel for the g-b redistribution, which explains the simultaneous fluctuation of occupation of the e sites with the redistribution. Thermal motion destabilizes the tetrahedral enclosure of protons, especially for those at the g sites being least constrained by the  $[Li_2Mg_2]$  tetrahedra.

The mean square displacement (MSD) curves of the hydrogens derived from longer NpT trajectories are shown in Figs. 2c and 2d. At 250 GPa and 25 K, proton diffusion other than g-b redistribution is rare, as shown by the almost flat gray curve. At higher temperatures, non-local proton motions become obvious, as revealed in the progressive increase of the MSD slope. At 300 GPa, the temperature-induced increase in MSD follows the same trend but with smaller values due to the more restricted proton motion in the structure. The average diffusion coefficient between 250 and 300 GPa at 140 K obtained from these curves is  $2.4 \times 10^{-7}$  cm<sup>2</sup>/s, which is remarkably the same order of magnitude as that measured for C15-Laves hydride solutions  $TaV_2H_x$  (x = 0.6 and 1.1) at ambient

conditions [29]. This agreement can be understood by recognizing that the proton diffusion is an equivalent to void diffusion moving in the opposite direction, analogous to the electron-hole equivalence in semiconductors, and the number of empty tetrahedral voids in a Li<sub>2</sub>MgH<sub>16</sub> formula unit is comparable to that of hydrogen sites in TaV<sub>2</sub>H<sub>x</sub> solutions. With increasing temperature, the calculated average diffusion coefficient increases to  $1.0 \times 10^{-6}$  cm<sup>2</sup>/s at 290 K and  $4.4 \times 10^{-6}$  cm<sup>2</sup>/s at 435 K.

To explore the nuclear quantum effects, we performed path integral molecular dynamics simulations [30] on Li<sub>2</sub>MgH<sub>16</sub> with 16 beads in the cubic cell of 152 atoms. It is clearly seen that proton is quantum diffusive at 30 K of both 250 and 300 GPa (Fig 2f and 2g), despite neglecting nuclear exchange. Proton distributions between neighboring hexagons suggest that the diffusion is non-local even at low temperature. Further ring polymer molecular dynamics gave average diffusion coefficients of 7.1×10<sup>-7</sup>, 3.1×10<sup>-6</sup> and 6.3×10<sup>-6</sup> cm<sup>2</sup>/s at 30, 150 and 300 K, respectively. The appreciable values indicate that the quantum diffusion persists to high temperatures. On the other hand, the values are a factor ~10<sup>2</sup> lower than the criterion for classical superionicity (~10<sup>-4</sup> cm<sup>2</sup>/s), *i.e.*, with protons diffusing freely within the structure [31]. The result suggests that proton diffusion is not strong enough to significantly change the statistical distribution of vibrational/electronic density of states predicted for Li<sub>2</sub>MgH<sub>16</sub>.

The atomic configurations of Li<sub>2</sub>MgH<sub>16</sub> were characterized by the average radial distribution function (RDF, g(r)) as shown in Fig. 3a for at 250 GPa and 290 K. Atomic vibrations eliminate the small gaps among the nearest inter- and intra-hexagon g-g, g-e and e-b separations of the initial structure, resulting in the formation of the first coordination shell of H peaked at ~1.1 Å, which nearly coincides with that found for LaH<sub>10</sub> at comparable conditions (190 GPa and 240 K). The position of this peak is almost unchanged with temperature from 140 to 435 K, but it shifts down to ~1.07 Å at 300 GPa. Comparing the RDFs in the Li<sub>2</sub>Mg sublattice to those for La in LaH<sub>10</sub> (Fig. S9 [32]) reveals that increased external pressure can compensate for the lower degree of 'pre-compression' by

smaller ions on condensing the H framework. Notably, proton diffusion in the  $Li_2Mg$  sublattice occurs at a much lower temperature than in the La sublattice of  $LaH_{10}$  (~800 K) [33]. This difference arises from the more flexible sublattice of interstitial sites of light elements and unsaturated occupation of those sites in  $Li_2MgH_{16}$ .

The vibrational density of states (VDOS) was calculated from the Fourier transform of the velocity autocorrelation functions [24], as shown in Fig. 3b for the 290 K and 250 GPa simulations. Proton diffusion results in a small but nonzero VDOS of H at zero frequency, with the value about 3% of the peak at 1563 cm<sup>-1</sup>, which is consistent with the small diffusion coefficients. The bonding interactions between neighboring atoms were also evaluated by the negative of Crystal Orbital Hamiltonian Population (COHP) integrals at the Fermi level  $\epsilon_F$  (denoted as f) [34]. We take the value of f for the H-H contact within the graphene-like layer ( $f_I$ ) and that between two adjacent layers ( $f_{II}$ ) using the oP48 structure for hydrogen phase IV at 0 K and 250 GPa as a strength measure [21]. The results indicate that the interactions in Li<sub>2</sub>MgH<sub>16</sub> at 290 K and 250 GPa can be roughly divided into three regions:  $\langle f_{II} \rangle \sim f_{II}$  and  $\langle f_I \rangle \sim f_{I$ 

The fluxional or diffusive nature of the H framework in these clathrate hydride structures have implications for calculations of their superconducting properties. As a first step in examining this, we estimated within a BCS framework the EPC constant  $\lambda$  for the H component of Li<sub>2</sub>MgH<sub>16</sub>, either neutral or charged with 0.25  $e^-$ /H, by the theory of Gaspari and Gyorffy [35], based on 16 uncorrelated configurations at 140/290 K and 250/300 GPa, and an approximation of all phonons by optical vibrations of hydrogen above 850 cm<sup>-1</sup>. The configurationally averaged  $\lambda$  fall in a range of 1.0-1.1 and 1.5-1.6 for the charged and neutral H frameworks, respectively. Although these values indicate strong EPC, they are smaller than that predicted for cubic LaH<sub>10</sub> (1.78-2.29) in the same pressure range at 0 K [14]. Assuming  $\mu^* = 0.1$ -0.13, configurationally averaged superconducting

 $T_c$ 's of 110-148 K and 176-245 K were obtained from the Allen-Dynes equation [36] for the charged and neutral H frameworks, respectively (Fig. 3d). These estimated  $T_c$ 's are below those predicted for the 'static', non-diffusive, structures (330-473 K) obtained by solving the Eliashberg equation (at 0 K) [27], they cover the temperature range over which we find strong classical and quantum diffusion.

Quantum and classical diffusion may occur in other superconducting superhydrides systems below  $T_c$ . Further simulations of coupled quantum diffusion and superconductivity, including the effect of the strong quantum behavior on pairing going well beyond BCS and other conventional models are required in order to obtain accurate predictions of superconducting critical temperatures for these materials.[20,37] As such, clathrate superhydrides, which contain a dense atomic hydrogen sublattice similar to that of atomic metallic hydrogen, provide a testable model for this behavior, as indicated by very recent results pointing to possible  $T_c$  well above room temperatures.[38]. The anticipated new phenomena invite continued experimental investigations that will advance our understanding of this novel class of quantum materials.

H. W. is thankful to Y. Ma and M. Shiga for valuable discussions. This work was supported by the National Natural Science Foundation of China (Grant No. 11974135, 11874176, 11774140, 11874175, 11974134, and 12074138), the Natural Sciences and Engineering Research Council of Canada, the China Postdoctoral Science Foundation under Grant No. 2016M590033, the Program for JLUSTIRT, and U.S. National Science Foundation (DMR-1933622; RJH). We used the computing facilities at the High-Performance Computing Centre of Jilin University and Beijing Super Cloud Computing Center.

H. W. and Y. Y. contributed equally to this work.

†wh@fysik.cn

†hanyuliu@jlu.edu.cn

## References

- [1] N. W. Ashcroft, Phys. Rev. Lett. 21, 1748 (1968).
- [2] N. W. Ashcroft, Phys. Rev. Lett. 92, 187002 (2004).
- [3] J. Bardeen, L. N. Cooper, and J. R. Schrieffer, Phys. Rev. 108, 1175 (1957).
- [4] L. Zhang, Y. Wang, J. Lv, and Y. Ma, Nat. Rev. Mater. 2, 17005 (2017).
- [5] A. R. Oganov, C. J. Pickard, Q. Zhu, and R. J. Needs, Nat. Rev. Mater. 4, 331 (2019).
- [6] T. Bi, N. Zarifi, T. Terpstra, and E. Zurek, in *Reference Module in Chemistry, Molecular Sciences and Chemical Engineering* (Elsevier, 2019).
- [7] C. J. Pickard, I. Errea, and M. I. Eremets, Annu. Rev. Condens. Matter. Phys. 11, 57 (2020).
- [8] J. A. Flores-Livas, L. Boeri, A. Sanna, G. Profeta, R. Arita, and M. Eremets, Phys. Rep. 856, 1 (2020).
- [9] A. P. Drozdov, M. I. Eremets, I. A. Troyan, V. Ksenofontov, and S. I. Shylin, Nature 525, 73 (2015).
- [10] M. Somayazulu, M. Ahart, A. K. Mishra, Z. M. Geballe, M. Baldini, Y. Meng, V. V. Struzhkin, and R. J. Hemley, Phys. Rev. Lett. **122**, 027001 (2019).
- [11] A. P. Drozdov, P. P. Kong, V. S. Minkov, S. P. Besedin, M. A. Kuzovnikov, S. Mozaffari, L. Balicas, F. F. Balakirev, D. E. Graf, V. B. Prakapenka, E. Greenberg, D. A. Knyazev, M. Tkacz, and M. I. Eremets, Nature **569**, 528 (2019).
- [12] P. P. Kong, V. S. Minkov, M. A. Kuzovnikov, S. P. Besedin, A. P. Drozdov, S. Mozaffari, L. Balicas, F. F. Balakirev, V. B. Prakapenka, E. Greenberg, D. A. Knyazev, and M. I. Eremets, (arXiv:1909.10482v1 (2019).
- [13] I. A. Troyan, D. V. Semenok, A. G. Kvashnin, A. V. Sadakov, O. A. Sobolevskiy, V. M. Pudalov, A. G. Ivanova, V. B. Prakapenka, E. Greenberg, A. G. Gavriliuk, V. V. Struzhkin, A. Bergara, I. Errea, R. Bianco, M. Calandra, F. Mauri, L. Monacelli, and R. Akashi, (arXiv:1908.01534).
- [14] H. Liu, I. I. Naumov, R. Hoffmann, N. W. Ashcroft, and R. J. Hemley, Proc. Natl. Acad. Sci. USA **114**, 6990 (2017).
- [15] F. Peng, Y. Sun, C. J. Pickard, R. J. Needs, Q. Wu, and Y. Ma, Phys. Rev. Lett. 119, 107001 (2017).
- [16] E. Snider, N. Dasenbrock-Gammon, R. McBride, M. Debessai, H. Vindana, K. Vencatasamy, K. V. Lawler, A. Salamat, and R. P. Dias, Nature **586**, 373 (2020).
- [17] W. Cui, T. Bi, J. Shi, Y. Li, H. Liu, E. Zurek, and R. J. Hemley, Phys. Rev. B 101, 134504 (2020).
- [18] Y. Sun, Y. Tian, B. Jiang, X. Li, H. Li, T. Iitaka, X. Zhong, and Y. Xie, Phys. Rev. B **101**, 174102 (2020).
- [19] H.-k. Mao and R. J. Hemley, Rev. Mod. Phys. 66, 671 (1994).
- [20] E. Babaev, A. Sudbø, and N. W. Ashcroft, Nature **431**, 666 (2004).
- [21] H. Liu and Y. Ma, Phys. Rev. Lett. 110, 025903 (2013).
- [22] R. P. Dias, O. Noked, and I. F. Silvera, Phys. Rev. Lett. 116, 145501 (2016).
- [23] A. F. Goncharov, I. Chuvashova, C. Ji, and H.-k. Mao, Proc. Natl. Acad. Sci. USA 116, 25512 (2019).
- [24] C. S. Zha, Z. Liu, M. Ahart, R. Boehler, and R. J. Hemley, Phys. Rev. Lett. 110, 217402 (2013).
- [25] H. Wang, J. S. Tse, K. Tanaka, T. litaka, and Y. Ma, Proc. Natl. Acad. Sci. USA 109, 6463 (2012).
- [26] H. Liu, I. I. Naumov, R. Hoffmann, N. W. Ashcroft, and R. J. Hemley, Proc. Natl. Acad. Sci. U.S.A. **114**, 6990 (2017).
- [27] Y. Sun, J. Lv, Y. Xie, H. Liu, and Y. Ma, Phys. Rev. Lett. 123, 097001 (2019).
- [28] A. V. Skripov, J. C. Cook, D. S. Sibirtsev, C. Karmonik, and R. Hempelmann, J. Phys.: Condens. Matter 10, 1787 (1998).

- [29] A. V. Skripov, J. Alloys Compd. 404-406, 224 (2005).
- [30] M. Shiga, in *Reference Module in Chemistry, Molecular Sciences and Chemical Engineering* (Elsevier, 2018).
- [31] E. Katoh, H. Yamawaki, H. Fujihisa, M. Sakashita, and K. Aoki, Science 295, 1264 (2002).
- [32] See Supplemental Material at <a href="http://link.aps.org/supplemental/xx.xxxx/PhysRevLett.xxx.xxxx">http://link.aps.org/supplemental/xx.xxxx/PhysRevLett.xxx.xxxx</a> for computational details, atomic trejactory, MSD, VDOS, and EDOS.
- [33] H. Liu, I. I. Naumov, Z. M. Geballe, M. Somayazulu, J. S. Tse, and R. J. Hemley, Phys. Rev. B **98**, 100102(R) (2018).
- [34] R. Dronskowski and P. E. Bloechl, J. Phys. Chem. 97, 8617 (1993).
- [35] G. D. Gaspari and B. L. Gyorffy, Phys. Rev. Lett. 28, 801 (1972).
- [36] P. B. Allen and R. C. Dynes, Phys. Rev. B 12, 905 (1975).
- [37] M. Y. Kagan and A. Bianconi, Condens. Matter 4, 51 (2019).
- [38] A. D. Grockowiak, M. Ahart, T. Helm, W. A. Coniglio, R. Kumar, M. Somayazulu, Y. Meng, M. Oliff, V. Williams, N. W. Ashcroft, R. J. Hemley, and S. W. Tozer, (arXiv: 2006.03004).

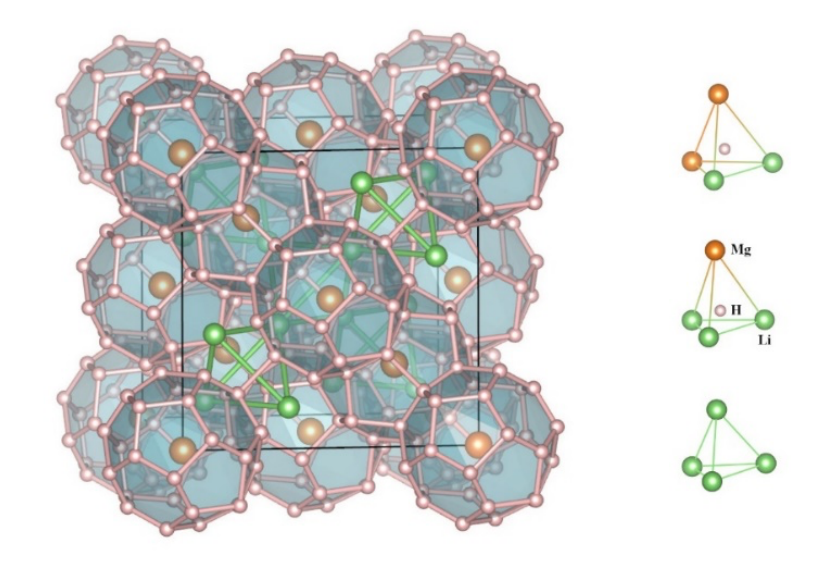


**FIG. 1.** (a) Clathrate structure of Li<sub>2</sub>MgH<sub>16</sub> (space group  $Fd\overline{3}m$ ).

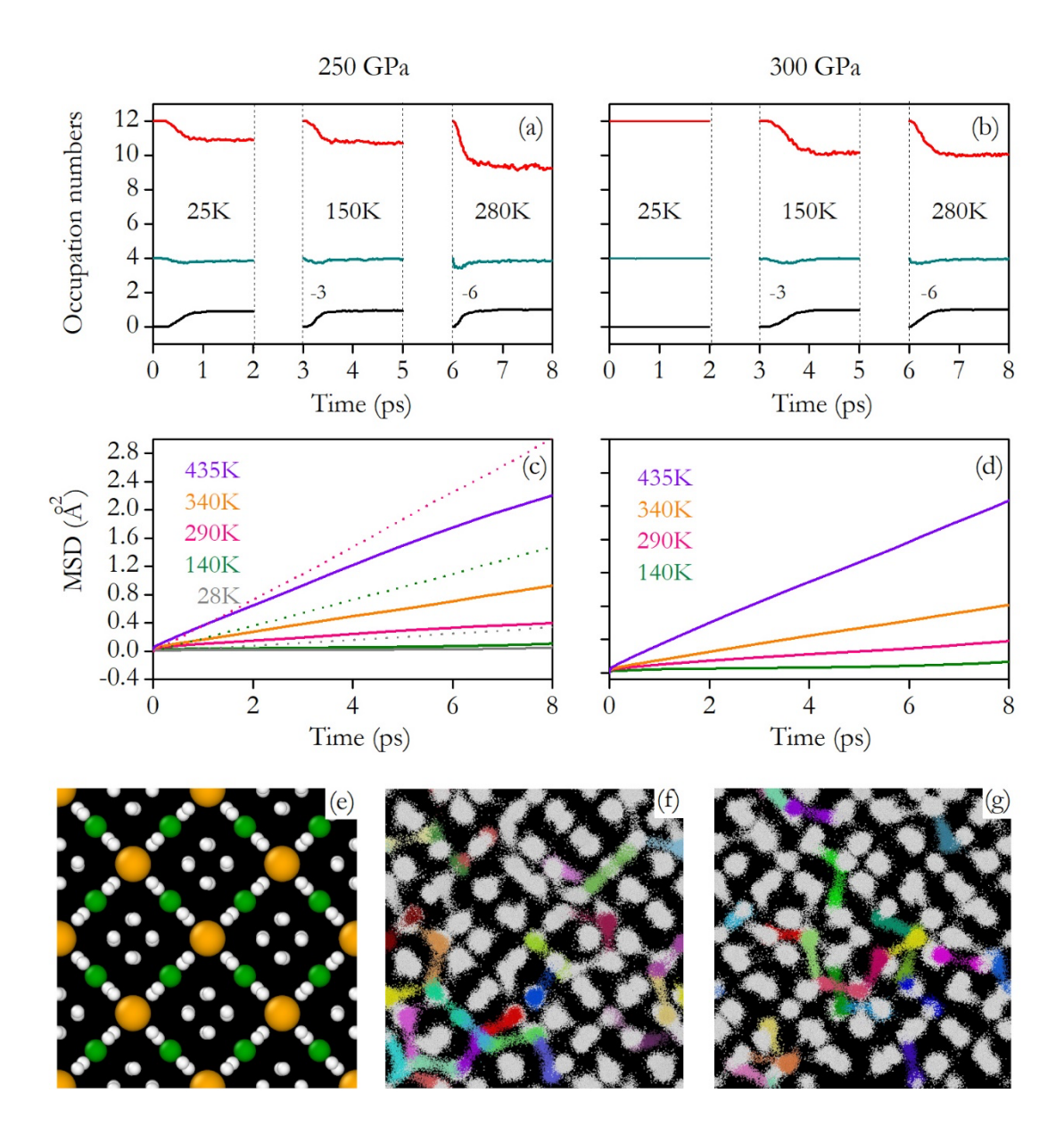


**FIG. 2.** (a)/(b) Occupation numbers of g (red), e (cyan), and b (black) sites. (c)/(d) The MSD of H component of Li<sub>2</sub>MgH<sub>16</sub> from MD (solid) at 28-435 K, and RPMD (dot) at 300 K (pink), 150 K (green) and 30 K (gray). (e) A side view of Li<sub>2</sub>MgH<sub>16</sub>. (f)/(g) Distribution of proton with 16 beads at ~30 K and 250/300 GPa from PIMD, with some protons marked by different colors.

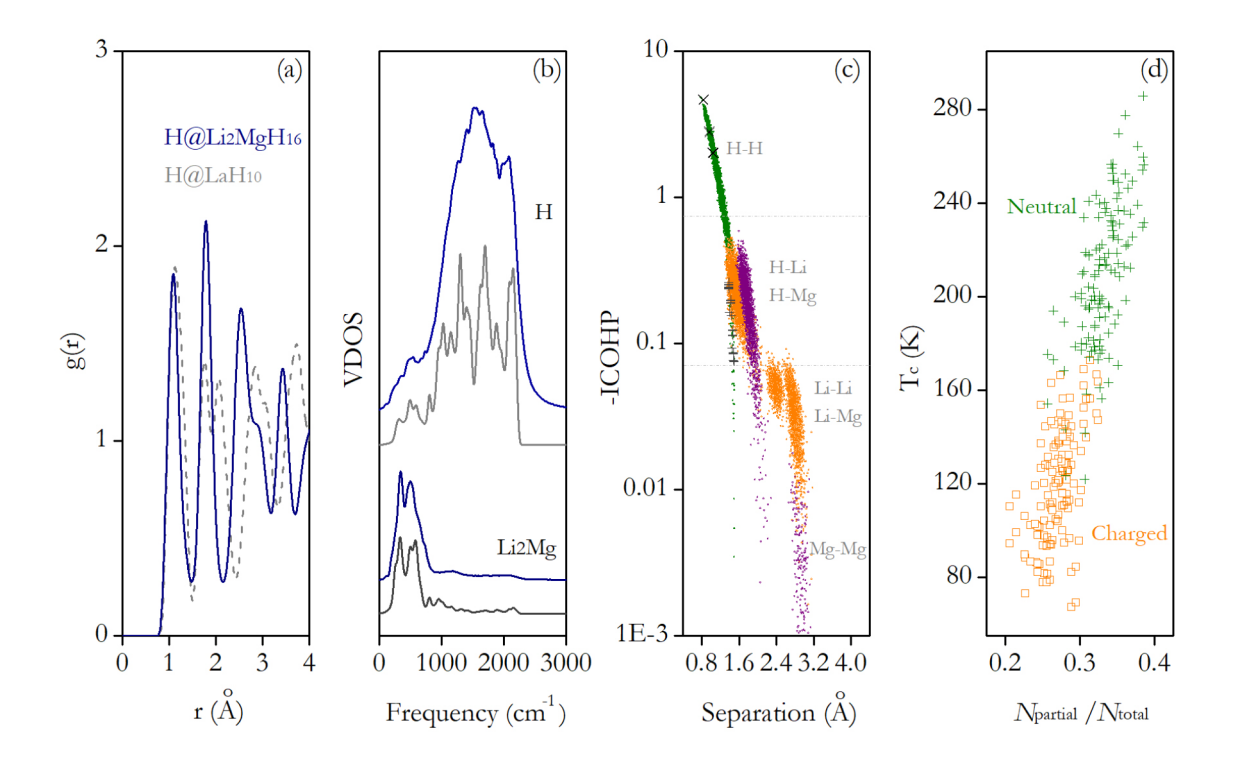


**FIG. 3.** (a) The g(r) of the H framework of Li<sub>2</sub>MgH<sub>16</sub> at 250 GPa and 290 K compared to that of LaH<sub>10</sub> at 190 GPa and 240 K. (b) VDOS of Li<sub>2</sub>MgH<sub>16</sub> at 290 K (blue) and 0 K (gray) at that pressure. (c) The I as a function of pair separations at 250 GPa and 290 K. (d) Configurationally distinguished I<sub>c</sub> as a function of partial-/total-I( $\epsilon_F$ ) of the H framework at 250-300 GPa and 140-290 K.